Forward-Looking Passive Radar With Non-Uniform Linear Array for Automotive Applications

Giovanni Paolo Blasone, *Member, IEEE*, Fabiola Colone, *Senior Member, IEEE*, and Pierfrancesco Lombardo, *Senior Member, IEEE*

***Abstract*—With the rapid and growing spread of automotive radar systems in modern vehicles, the problem of their mutual interference is becoming a major safety concern. This article considers the use of receive-only sensors onboard the vehicles, which exploit an external illumination source to provide automotive radar functionalities. The passive radar paradigm would solve the problem of mutual interference, allowing different systems to share the same transmitted signal. A preliminary analysis of the feasibility of this concept is carried out, exploiting real-world transmitters of opportunity. The potentialities offered by both satellite and ground-based illuminators are investigated and the expected performance is evaluated in terms of achievable coverage and spatial resolution. Aiming to enable a practical implementation of the proposed concept, an appropriate signal processing scheme is proposed to obtain maps of the observed scene. A Doppler beam sharpening approach is adopted to discriminate and localize stationary scatterers in azimuth based on the differences in their relative Doppler shift. The problem of left/right ambiguity arising from the forward-looking geometry is tackled by exploiting an array of few antenna elements on receive. Specifically, an ambiguity removal approach is proposed, based on digital beam pattern adaptation, designed to maximise the response in the desired direction and suppress unwanted echoes from the corresponding ambiguous one. The effectiveness of this approach is further improved by cascading an apodization technique that prevents the undesirable increase in the noise level. Moreover, some criteria are introduced for the design of the antenna layout, resorting to non-uniform linear array configurations. The proposed system is tested against a simulated environment, where the multi-channel signal processing, combined with a properly designed array layout, is shown to provide an unambiguous mapping of the observed scene over wide angular sectors, even operating with few antenna elements on receive.**

***Index Terms*—Automotive radar, passive radar, Doppler beam sharpening, left/right ambiguity resolution, NULA.**

I. Introduction

THE last decades have seen a pervasive and ever-increasing diffusion of the radar technology in the automotive sector. Modern vehicles are equipped with multiple sensors designed to provide essential safety and comfort features and to enable advanced driver assistance systems (ADAS), and autonomous driving functionalities. Radar is the core sensing technology, being able to sense the environment also in harsh conditions (poor lighting, adverse weather, etc.), to detect the objects in the vicinity of the vehicle, and to accurately measure their speed and range. Most automotive radar systems operate in the frequency band 76-81 GHz, employing frequency modulated continuous wave (FMCW) signals [1]. They usually transmit wideband waveforms to ensure range resolutions below one meter, and they are typically required to cover from few tens of meters (short-range) up to few hundreds of meters (long-range), depending on the specific application.

As the number automotive radar transceivers operating on the road is foreseen to rapidly increase over the coming years, the problem of mutual interference between them is expected to become an important issue [2], [3], [4]. The mutual interference can largely affect the capabilities of the sensors and degrade their performance, for instance by increasing the disturbance level, compromising target detection, generating ghost targets, or even causing a complete loss of the radar functionality.

Therefore, automotive radar mutual interference is going to become a critical safety concern and has motivated several studies aimed at mitigating or avoiding it, making this topic a very important area of research for the long-term development of ADAS and autonomous driving. A demonstration of this is the great attention by both the automotive industry and the research community, and the numerous contributions of the recent years on this subject [5], [6], [7], [8], [9], [10], [11], [12], [13], [14], [15].

Several solutions have been proposed to face the problem of mutual interference. Most of the published studies focus on the attenuation or removal of the interference after it has been revealed at the receiver [7], [8], or by employing compressive sensing techniques [9]. Other approaches aim to mitigate or avoid the interference exploiting waveform diversity. The probability of overlap can be diminished by properly varying the waveform parameters, according to temporal, frequency, or code multiplexing strategies. The FMCW and orthogonal frequency division multiplexing (OFDM) waveforms have been considered and compared under interference conditions [10], [11], [12]. Strategies were proposed to adjust the waveform parameters by randomisation [13], cognitive approaches [14], or partial coordination among the systems [15]. Nevertheless, due to the nature of these solutions, the interference mitigation

Manuscript received 16 August 2022; revised 3 January 2023; accepted 16 March 2023. Date of publication 13 April 2023; date of current version 19 September 2023. This work was supported by the European Union thorugh the Italian National Recovery and Resilience Plan (NRRP) of NextGenerationEU, partnership on Telecommunications of the Future under Grants PE00000001 - program "RESTART", and CUP B53C22004050001. The review of this article was coordinated by Prof. Hongzi Zhu. *(Corresponding author: Fabiola Colone.)*

The authors are with the Department of Information Engineering, Electronics and Telecommunications, Sapienza University of Rome, 00184 Rome, Italy (e-mail: giovannipaolo.blasone@uniroma1.it; fabiola.colone@uniroma1.it; pierfrancesco.lombardo@uniroma1.it).

Digital Object Identifier 10.1109/TVT.2023.3266789

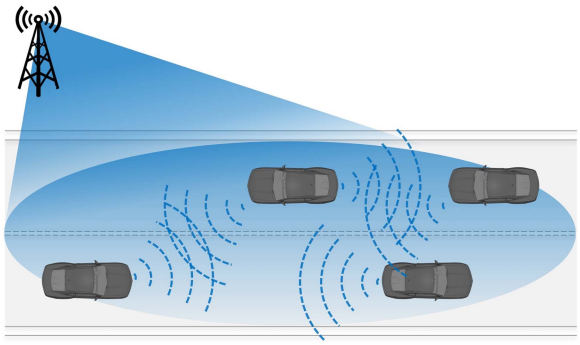

Fig. 1. Automotive passive radar sensors sharing an external transmitter as an illuminator of opportunity.

performance worsens as the number of sensors increases, and the orthogonality of waveforms can only be preserved with a limited number of active radar units.

To overcome the above limitations, this work proposes an unconventional approach, which starts from a totally different perspective. We investigate the idea of employing a receive-only sensor onboard the vehicle, which exploits an available external illumination source in bistatic configuration. The passive radar paradigm would permit different radar systems to share the same transmitted signal, thus eliminating the problem of mutual interference (see Fig. 1). Such an external source might be a third-party non-cooperative transmitter, such as those employed for broadcast communications, or a transceiver station from a mobile communication network, or even a dedicated or partially dedicated signal transmitted by upcoming vehicle to infrastructure communication systems [16], [17], [18], [19]. This solution goes in the direction of a more efficient use of the spectrum and towards the coexistence of communication and sensing. Specifically, in the perspective of an integrated sensing and communication (ISAC) system, the transmitted waveform might be designed so as not only to accomplish its primary function but also to have convenient properties for radar purposes.

Apparently, the downsides of a passive radar solution are due to its reliance on an external illumination source, which rises numerous non-negligible challenges. The reliability and performance of the system would depend on the parameters of the exploited transmitter and the characteristics of the waveform. Likewise, they might be strongly affected by the illumination condition and the time-varying bistatic geometry. Therefore, a suitable strategy for the selection of one or more sources of opportunity, among the several available nowadays and in the next future, would be essential to meet the required safety standards. In addition, appropriate signal processing techniques and operational strategies are needed to tackle the main limitations of a mobile passive radar scenario.

Recently, significant advances have been made in the context of passive radar systems onboard moving platforms. Numerous proofs of concept and experimental validations, carried out from both ground-based and aerial platforms, have demonstrated the feasibility of this technology, showing encouraging results in both surveillance [20], [21], [22], [23] and imaging [24], [25] applications.

In this work, a preliminary study is carried out, aimed at investigating the feasibility of an automotive passive radar for the detection and localization of obstacles in the vicinity of the moving vehicle, along the line preliminarily presented in [26]. The attention is mainly focused on the use of non-cooperative transmitters and different today's commonly available sources are taken into account as potential illuminators of opportunity. By way of example, a digital video broadcasting – satellite (DVB-S) transmitter is primarily considered. The particular interest in geostationary satellite illuminators is motivated by the wide and stable coverage they can offer. Moreover, this choice is also fostered by the recent advances and inspiring results of the DVB-S based passive radar technology for short-range surveillance applications, as evidenced by the numerous recent contributions on this topic [27], [28], [29], [30].

First, the proposed passive radar system concept is illustrated, analysing its feasibility in terms of expected coverage and achievable spatial resolution performance. The basic signal processing scheme needed for its implementation is described. In particular, based on the knowledge of the receiver motion, and assuming to process a sufficiently short coherent integration interval, the ability to resolve and localize fixed scatterers in the azimuth direction is obtained exploiting a simple Doppler beam sharpening (DBS) approach.

Then, the problem of left/right ambiguity arising from the forward-looking observation geometry is addressed. In fact, scatterers located symmetrically around the direction of motion are characterized by the same Doppler shift, which results in an ambiguous mapping of the observed scene. To solve this problem and correctly associate each scatterer to its angular direction, a multichannel processing approach is proposed, based on the availability of multiple receiving antennas displaced in the direction orthogonal to the motion. Due to the typical restrictions in terms of compactness and cost of the system, and to the considerably lower frequency bands of the common illuminators of opportunity compared to those used in conventional automotive radar, a limited number of channels is expected to be available for the passive radar. This would result in array patterns with relatively large beams, making the simple spatial selectivity of an array beam steering inadequate to resolve the left/right ambiguity. Therefore, a spatial filtering algorithm is proposed, based on digital beamforming and array-based directional nulling techniques, which maximises the response in the desired direction and simultaneously suppresses potential echoes from the corresponding ambiguous one. Moreover, proper design criteria for a strategic positioning of the few antenna elements are proposed, based on non-uniform linear array (NULA) configurations. They are aimed at improving the effectiveness of the left/right ambiguity removal algorithm in all the angular sector of interest, allowing an unambiguous mapping of all the scatterers in the observed area. In addition, an apodization technique is suggested, with the purpose of preventing an undesirable increase in the noise level.

Finally, the effectiveness of the proposed solutions and the ability of the system to resolve stationary scatterers in the vicinity of the vehicle and correctly locate them with respect to the receiver position are verified in a simulated scenario.

The structure of the article is as follows. Section II provides an overview of the considered system concept, followed by the analysis of the expected coverage and spatial resolution capabilities, and a detailed description of the proposed signal processing scheme. The algorithm for the left/right ambiguity removal and the considerations on the design of the array are provided in Section III. Section IV reports the results obtained in a simulated scenario. Finally, our conclusions are drawn in Section V.

II. System Concept and Feasibility Analysis

In this section, the concept of an automotive passive radar is first introduced, as a possible solution to the problem of mutual interference. The potentialities of this concept, its main challenges, and the possible illuminators of opportunity are discussed (Section II-A). A power budget study is presented, which demonstrates the feasibility of the concept in a practical scenario, assuming some commonly available terrestrial and satellite sources (Section II-B). Thereafter, an outline of the architecture and signal processing chain required to implement the proposed passive radar system is introduced (Section II-C). Finally, the achievable spatial resolution is analysed, with reference to possible automotive radar tasks, pointing out the open issues to be considered, with special attention to the forward-looking radar configuration (Section II-D).

A. System Overview and Potential Illuminator of Opportunity

The considered system consists of a passive radar receiver installed on a ground moving vehicle and exploiting the signal emitted by an external illuminator of opportunity to perform automotive radar tasks, such as the detection and localization of potential obstacles in the vicinity of the vehicle. The idea of using a receive-only sensor to provide automotive radar functionalities meets the growing need to reduce the mutual interference between radar units. This solution, in fact, would allow the radar system to sense the surrounding environment without transmitting its own signal. The exploited illuminator might be shared by multiple different radar units, eliminating the chance of interference. The resulting system may represent an auxiliary or backup solution to rely on in the condition of particularly congested environments, provided that its cost and size are kept small.

The proposed passive radar concept must face a number of challenges, mostly attributable to the reliance on an external illumination source. First, the transmitted waveform must be known at the receiver for a correct signal range compression. In addition, the signal characteristics and ambiguity function may not be particularly suitable for radar purposes. Moreover, the performance of the system would be dependent on the parameters of the exploited transmitter, the illumination conditions and the bistatic geometry, as well as affected by the typical passive radar restrictions in terms of complexity and number of receiving channels. While some of the above issues have been addressed by the recent research on mobile passive radar for the case of surveillance and imaging applications, specific signal processing techniques and methodologies need to be developed for the considered automotive scenario.

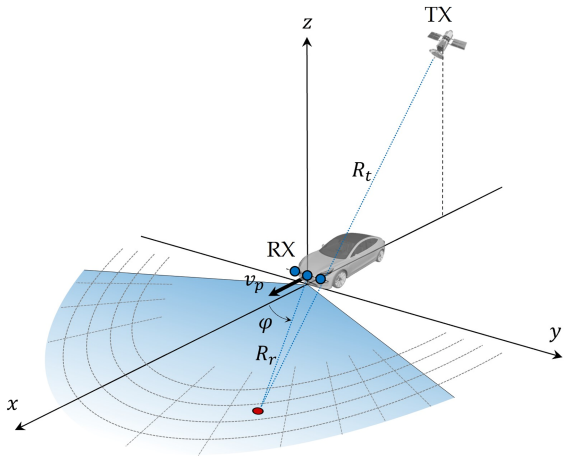

Fig. 2. System geometry of a satellite-based passive automotive radar. The blue circles represent the radar receiving antennas, organized in a linear array (either ULA or NULA) in a forward-looking configuration.

The selection of suitable illuminators of opportunity is also a critical aspect. An effective source should be characterized by a large-scale availability, a reliable illumination, and a wide bandwidth. Different possible solutions can be considered: non-cooperative transmitters, such as those used for terrestrial and satellite broadcast communications; transceivers stations from mobile communication networks; dedicated emitters or ISAC systems connecting vehicle with each other and with infrastructures. In this preliminary study, the case of non-cooperative transmitters is analysed, focusing on today's commonly available sources. By way of example, a ground-based 5G transceiver and a satellite-based DVB-S transmitter are considered as potential illuminators of opportunity. In fact, these choices are characterized by relatively wide bandwidths and high carrier frequencies, which are essential features to ensure high range and velocity resolution capabilities. In particular, the DVB-S signal transmitted by a geostationary satellite may offer a stable and reliable illumination, which is commonly available on a very large scale with a favourable geometry, less subject to shadowing phenomena, at least in an open-space environment.

A sketch of the bistatic system configuration is depicted in Fig. 2, where the case of a satellite transmitter is shown. The vehicle is assumed to move in a straight line along the x-axis at velocity v_p. The exploited transmitter is supposed to be stationary and, for simplicity, located in the opposite direction to the direction of motion of the receiver. The radar antenna is assumed mounted in a forward-looking configuration and collects the echoes from the scatterers surrounding the vehicle, within a given region of interest. The observed area is supposed to be limited to a front angular sector, i.e., $\varphi \in [-\varphi_{max}, \varphi_{max}]$, where φ denotes the azimuth angle on the ground plane, with respect to the x-axis.

TABLE I
TRANSMITTER AND RECEIVER SYSTEM PARAMETERS

Parameter	Symbol	DVB-S	5G (FR1)	5G (FR2)
Carrier frequency	f_0	11 GHz	3.5 GHz	24 GHz
EIRP	$EIRP$	53 dBW	23 dB	5 dB
TX distance	R_t	37600 km	2 km	250 m
TX incidence angle	θ_t	42°	88°	88°
Signal bandwidth	B	30 MHz	50 MHz	100 MHz
RX antenna gain	G_r	16 dB		
RX noise figure	F	5 dB		
Propagation loss	L_0	3 dB		
Target RCS	σ_t	[1,5,10] m^2		
Platform velocity	v_p	13 m/s		
CPI	T_i	0.1 s		

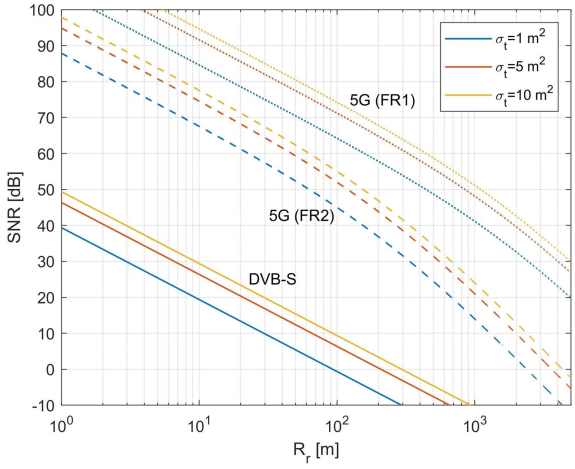

Fig. 3. Expected signal to noise ratio as a function of the receiver to scatterer distance for different possible values of the scatterer radar cross section.

B. Expected Coverage

To investigate the feasibility of the proposed system, its coverage capabilities are first analysed. A power budget study is carried out using a reference example: a geostationary satellite-based transmitter is considered as an illuminator of opportunity, at approximately 37000 km from the observed scene. The main parameters assumed for the exploited transmitter and for the radar system are listed in Table I.

Specifically, a DVB-S transmission is assumed available, with carrier frequency $f_0 = 11\ GHz$ (Ku band), frequency bandwidth $B = 30\ MHz$ and effective isotropic radiated power $EIRP = 53\ dBW$. The selected parameters represent typical values of common DVB-S downlink transmissions.

For the receiving antenna, a gain $G_r = 16\ dB$ is assumed. Such value is reasonable for an antenna whose half-power beamwidth covers approximately 60° in azimuth and 15° in elevation. A receiver noise figure $F = 5\ dB$ and additional propagation losses $L_0 = 3\ dB$ are considered.

The expected signal to noise power ratio (SNR) of an echo from a target with a radar cross section (RCS) σ_t, measured after the signal processing stages for waveform compression, is given by the bistatic range equation

$$SNR = \frac{EIRP\ G_r\ \lambda^2\ \sigma_t\ T_i}{(4\pi)^3\ R_t^2\ R_r^2\ k_B T_0 F L_0} \tag{1}$$

where R_r and R_t are respectively the target to receiver and to transmitter distance; T_i indicates the length of the coherent processing interval (CPI); λ denotes the signal wavelength; T_0 is the noise temperature and k_B the Boltzmann constant.

Fig. 3 reports the achievable target SNR resulting from (1), for different possible values of σ_t, as a function of the receiver to scatterer distance R_r. A CPI length $T_i = 0.1\ s$ is assumed. The relatively short integration interval makes it possible, to a first approximation, to neglect the migration effects, as well as to provide a sufficiently fast update time to the radar system.

As expected, due to the significant distance of the assumed transmitter, the results of Fig. 3 show that the range coverage capability of the system would be relatively limited. For 10 m^2 targets, an SNR of 10 dB could be achieved up to 100 m. For smaller targets, 1 m^2 and 5 m^2, this distance reduces to 30 m and 70 m, respectively. Anyway, such an order of distances might be compatible with some standard automotive radar applications, which is a promising result. In principle, short to medium range radar tasks might be enabled, such as, for instance, obstacle detection and collision warning.

In addition, the achievable performance might be further improved, by extending the considered integration time and the related processing complexity, by increasing the gain of the receiving antenna, by exploiting alternative sources of opportunity, or even by integrating the results obtained from multiple transmitters, where available.

A much higher power density is expected to be available from ground-based illuminators of opportunity, such as those offered by the widespread 5G networks, potentially enabling a wider coverage. Assuming to exploit the signal emitted by a 5G transmitter, the above power budget analysis is repeated. Specifically, two possible frequency ranges are considered, 3.5GHz and 24 GHz, respectively denoted as FR1 and FR2. The main parameters assumed are also listed in Table I and are consistent with the typical characteristics of 5G emitters. The results are reported in Fig. 3. As expected, a considerably improved range coverage can be achieved exploiting 5G transmitters, with respect to a DVB-S based solution. Such a level of coverage might be sufficient for most of the automotive radar applications, up to far-range. Comparing the two frequency bands, the FR2 offers a larger bandwidth, and therefore a better expected range resolution, but also a lower average transmitted power, which results in a reduced coverage, compared to FR1.

Noticeably, exploiting this kind of illuminators rises several non-negligible challenges, such as dealing with typically strongly multiuser scenarios, spatially directive and temporally discontinuous transmissions, and instantaneous bandwidth variations. Recently, a first example of a practical 5G network-based passive radar scenario was shown in [33].

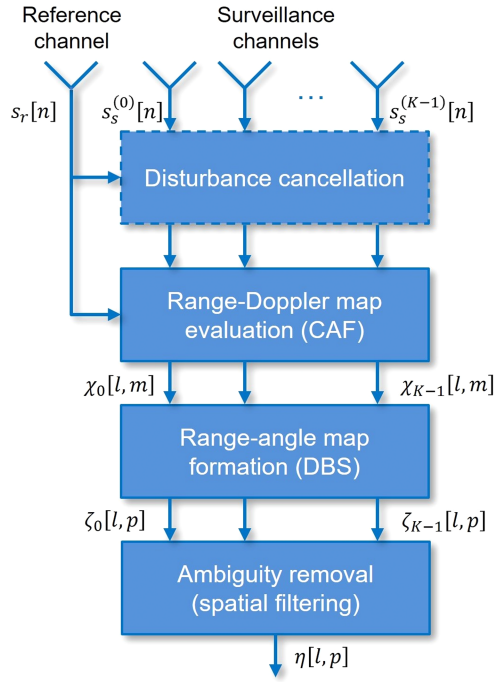

Fig. 4. Sketch of the proposed passive radar processing scheme.

By way of illustration, in the reminder of this study, the attention will be focused on the use of DVB-S as an illuminator of opportunity. Note that, in addition to the large-scale availability of the satellite-based illumination, and the maturity of the passive radar solutions exploiting this kind of signal, the DVB-S carrier frequency also represents an intermediate case among those mentioned.

C. Proposed Signal Processing Scheme

The signal processing chain proposed to implement the considered passive radar system is depicted in Fig. 4. The case of K surveillance channels is assumed, and below we describe the processing steps applied to each of them to obtain maps of the observed scene. In Section III, the availability of multiple channels on receive will be exploited for ambiguity removal.

A clean replica of the transmitted signal is assumed to be available at the receiver, either collected by a dedicated reference channel or obtained by means of a decode/recode approach. For digital transmissions, also the exploitation of a-priori known portions of the signal could be considered.

The resulting reference and surveillance signals undergo a conventional passive radar processing chain. First, depending on the level of the direct signal contribution at the surveillance antenna, and on the ambiguity function of the exploited waveform, a direct signal interference removal stage might be required to enable the final detection of targets [31].

Then, the range-Doppler map is evaluated by computing the cross-ambiguity function (CAF) between the reference and the surveillance signal, which corresponds to a matched filtering operation, providing the estimates of the bistatic range and bistatic Doppler shift of each potential target echo.

The bistatic range is defined as $R_b = R_r + R_t - r_b$, where r_b is the receiver to transmitter baseline. Since the transmitter is assumed stationary, the bistatic Doppler frequency of a fixed scatterer is obtained by the projection of the receiver velocity vector on the receiver to scatterer line of sight. For a ground scatterer it can be expressed as

$$f_D = \frac{v_p}{\lambda} \cos\varphi \tag{2}$$

Denoting with $s_r[n]$ and $s_s^{(i)}[n]$, $n = 0, \ldots, N-1$ and $i = 0, \ldots, K-1$, respectively the samples of the reference signal and surveillance signal at the i-th channel, the output of the CAF at the generic range-Doppler bin is given by

$$\chi_i\ [l,m] = \sum_{n=0}^{N-1} s_s^{(i)}\ [n]\ \overline{s_r}\ [n-l]\ e^{-j2\pi\frac{mn}{N}} \tag{3}$$

where $N = \lfloor f_s T_i \rfloor$ is the number of integrated samples in the CPI, f_s being the sampling frequency; l and m represent the range and Doppler bin indexes, respectively, corresponding to bistatic range $R_b\ [l] = l\ \delta\ R_b = l(c/B)$ and bistatic Doppler shift $f_D\ [m] = m\ \delta\ f_D = m/T_i$; the overline denotes the complex conjugate operation.

Several sub-optimal algorithms have been proposed in the literature, which provide an efficient implementation of (3) based on discrete Fourier transform (DFT) [31]. In this work, a batch processing architecture is assumed, where the CPI is fragmented in batches that are individually range compressed and Doppler processed in the equivalent slow-time dimension.

Notice that the CPI length T_i affects the achievable SNR in (1), as well as the Doppler frequency resolution δf_D: the longer the integration time, the higher the range coverage and the finer the Doppler frequency resolution, at the expense of computational complexity and potential migration effects.

Therefore, the resolution in Doppler frequency is exploited by the system to achieve an angular discrimination capability in the azimuth direction. Making use of the relationship between the azimuth angle and the Doppler shift of stationary scatterers, the range-Doppler map can be converted into a range-angle map, where the potential detections can be angularly localized. This step is described more in detail in the next subsection, where the range and azimuth resolution capabilities are analysed.

D. Expected Spatial Resolution

As known, the resolution in bistatic range is determined by the frequency bandwidth of the exploited signal and is given by $\delta R_b = c/B$. The equivalent monostatic range resolution achievable on the ground plane δR_g depends on the bistatic observation geometry and can be evaluated as, [34]

$$\delta\ R_g = \frac{c/B}{\|\boldsymbol{P}_g \nabla R\|} = \frac{c/B}{\|\boldsymbol{P}_g\ (\boldsymbol{u}_r + \boldsymbol{u}_t)\|} \tag{4}$$

where $\nabla R = \nabla(R_r + R_t)$ is the gradient of the total bistatic range, being $\nabla\ () = [\frac{\partial}{\partial x}, \frac{\partial}{\partial y}, \frac{\partial}{\partial z}]$; $\boldsymbol{u}_r$ and $\boldsymbol{u}_t$ represent the unit vectors of the receiver to scatterer and transmitter to scatterer line of sight, respectively, while $\boldsymbol{P}_g$ denotes the projection operator on the ground plane and $\|\|$ the Euclidean norm.

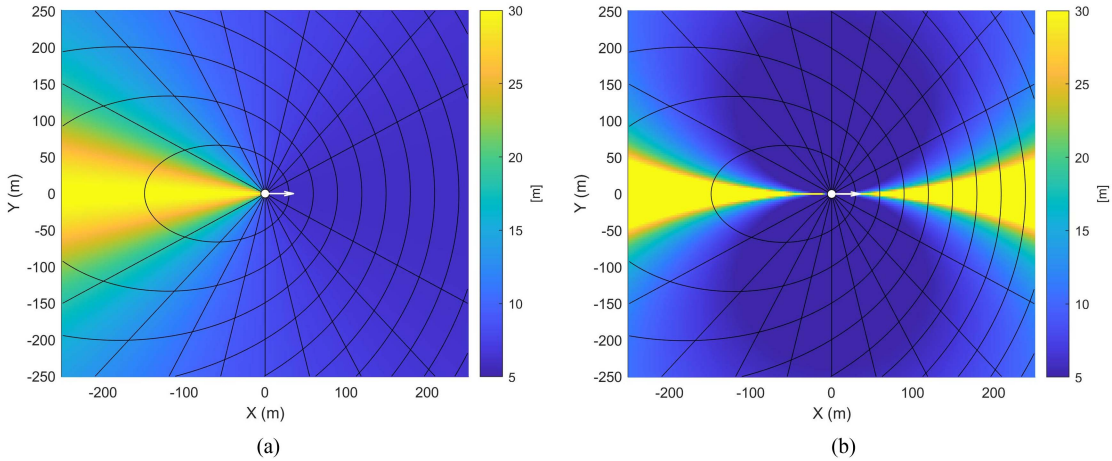

Fig. 5. Expected ground spatial resolution: (a) Range resolution; (b) azimuth resolution. The black curves represent the bistatic iso-range and iso-Doppler lines. The white arrow indicates the front radar's direction of driving. The system parameters reported in Table I are assumed, for the case of a DVB-S illuminator of opportunity. The assumed bistatic geometry is the one depicted in Fig. 2, with the transmitter located behind the receiver. For different geometries, the achievable range resolution would rotate and slightly change depending on the direction and incidence angle of the transmitter, respectively (see (4)). Since the transmitter is stationary, the azimuth resolution is determined only by the receiver's velocity vector (see (6)).

Fig. 5(a) shows the expected ground range resolution for the DVB-S case study considered in Table I. Because of the assumed bistatic geometry and the nonzero grazing angle of the transmitter, a range resolution just slightly worse than 5 m is obtained in the front region, which includes the observed area. In the opposite direction (in direction of the transmitter), the resolution degrades as expected, since the geometry gets close to the forward scatter condition.

The resolution in Doppler frequency is instead given by the inverse of the CPI duration, namely $\delta f_D = 1/T_i$. Making use of the known relationship between the observation angle and the Doppler shift for stationary scatterers, as expressed in (2), the Doppler frequency resolution can be mapped into an angular resolution. In particular, under the hypothesis of a sufficiently short CPI and a not excessively high velocity of the platform, the quadratic term in the scatterer phase history can be neglected. This allows to resolve and localise scatterers in azimuth based on the differences in their relative Doppler shift through an efficient Doppler beam sharpening (DBS) approach, [35]. Clearly, this approach requires the radar system to be in motion and this motion to be known.

Assuming a negligible variation of the Doppler frequency gradient ∇f_D within the CPI, the spatial resolution in azimuth achievable on the ground plane can be approximated as, [34]

$$\delta a_g \cong \frac{1/T_i}{\|\boldsymbol{P}_g \nabla f_D\|} = \frac{\lambda/T_i}{\left\|\boldsymbol{P}_g \frac{\partial}{\partial t} \nabla R\right\|} = \frac{\lambda/T_i}{\left\|\boldsymbol{P}_g \frac{\partial}{\partial t} (\boldsymbol{u}_r + \boldsymbol{u}_t)\right\|} \tag{5}$$

In the considered case study, where the transmitter is stationary and the altitude of the receiver is negligible, the azimuth resolution in (5) can be further simplified to

$$\delta a_g \cong \frac{\lambda\, R_r}{v_p T_i \sin\varphi} \tag{6}$$

Fig. 5(b) shows the expected ground azimuth resolution for the DVB-S case study reported in Table I. A fine resolution is obtained in the ranges of interest, with values comparable to the corresponding range resolution, for observed directions that are sufficiently far from the motion direction. Conversely, the azimuth resolution rapidly deteriorates when getting closer to the along-track direction, because of the nonlinear mapping between Doppler and angular resolution. Nevertheless, it is worth noting that, despite the limited azimuth discrimination capability in the front region, scatterers located in front of the vehicle can still be detected and resolved in range.

In principle, a 2D mapping in the range and angle domain could be effectively achieved if the antenna pointing direction on receive is squinted with respect to the along track direction and its directivity limits the observed sector so that it does not include the forward-looking direction, [26]. Conversely, if the proposed approach is applied in a forward-looking geometry, where the radar antenna observes a front angular sector, it does not allow to discriminate between the left and right direction, thus resulting in an ambiguous mapping of the observed scene.

In this case, the range-angle map at the i-th channel can be obtained from the corresponding range-Doppler map as

$$\begin{aligned} \zeta_i\ [l,p] &= \chi_i\ [l, M-|p|] \\ l &= 0,\ldots,L-1 \\ p &= -M+1,\ldots,0,\ldots,M-1 \end{aligned} \tag{7}$$

where indexes l and p respectively define the bistatic range and the azimuth angle indices. Note that, for each Doppler frequency bin of interest, limited to positive values in the considered forward-looking configuration, two angles are identified according to (2), which can be expressed as $\varphi\,[p] = -\varphi\,[-p] = \text{acos}(f_D[M-|p|]\lambda/v_p)$.

An example is shown in Fig. 6, where the case of a single scatterer is assumed. As expected, the radar is not able to uniquely associate the scatterer Doppler frequency (Fig. 6(a)) to its actual angular direction, resulting in the presence of an ambiguous replica of the scatterer in the range-angle map (Fig. 6(b)).

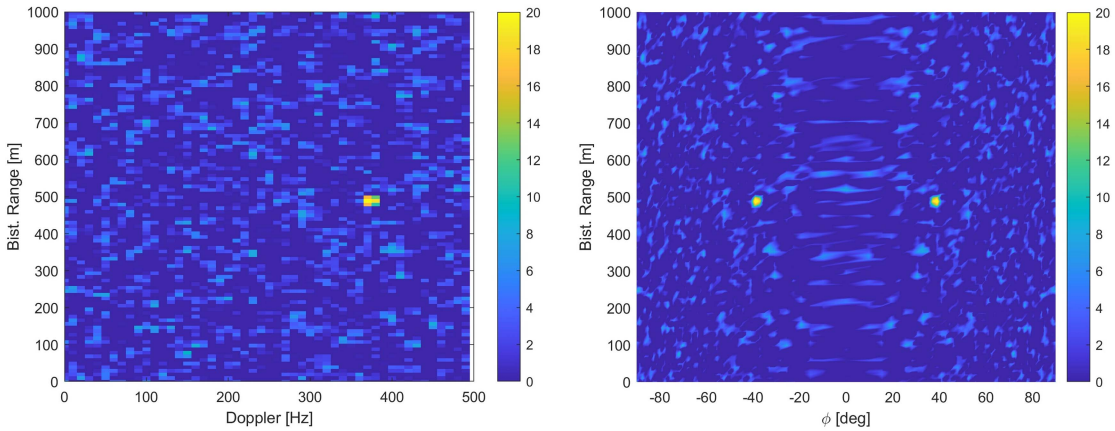

Fig. 6. Simulated example with a single scatterer showing the effect of the left/right ambiguity when operating DBS in a forward-looking radar configuration: (a) Bistatic range-Doppler map; (b) corresponding range-angle map. The same parameters of Table I for the case of a DVB-S illuminator were assumed.

This problem is addressed more in detail in Section III, where an algorithm for the removal of left/right ambiguity based on multichannel signal processing is proposed.

Although the expected spatial resolution in the considered case study seems slightly worse than that typically foreseen in common automotive applications, it may still provide useful information for the safety of the vehicle. Furthermore, better performance could be sought making different choices for the system parameters, architecture, and processing strategies. A finer range resolution would require a larger signal bandwidth, which could be achieved, for instance, by acquiring multiple transmitted DVB-S channels. On the other hand, a longer integration time, combined with proper synthetic aperture radar (SAR) focusing techniques, could significantly improve the achievable resolution in the azimuth direction. These improvements are not further explored in the following. Rather, this article mainly aims to introduce and demonstrate the proposed solutions to provide an unambiguous imaging of the area in front of the vehicle.

III. Ambiguity Removal by Multichannel Processing

In the considered forward-looking configuration, where the area observed by the moving receiver corresponds to a front angular sector, scatterers located symmetrically around the direction of motion are characterized by the same Doppler shift. This results in a left/right ambiguity problem. Namely, each Doppler frequency bin of interest within the interval $f_D \in [f_D^{\min}, f_D^{\max}]$ corresponds to two possible azimuth directions. Note that $f_D^{\max} = v_p / \lambda$ is associated to the forward-looking direction $\varphi = 0°$, while $f_D^{\min}$ is given by the upper and lower bounds of the observed angular sector.

To resolve the left/right ambiguity, a spatial filtering algorithm is proposed, based on digital beamforming and directional nulling. The algorithm is first introduced assuming a uniform linear array (ULA) configuration (Section III-A). Then, the use of NULA is proposed to improve the ambiguity removal performance for angles close to the motion direction, in the case of a limited number of available receiving channel (Section III-B). Finally, an additional non-linear signal processing strategy is presented, to improve the performance obtained with the optimized NULA (Section III-C).

A. Left/Right Ambiguity Removal

In order to correctly associate each scatterer to its angular direction, we need to solve the ambiguity between the couple of angles associated to each Doppler frequency bin. This can be accomplished by exploiting the availability of multiple receiving channels, displaced in the direction orthogonal to the receiver motion. The resulting array pattern can be optimized by a digital beamforming in order to maximise the response in the desired direction and simultaneously minimise it in the corresponding ambiguous one.

For this purpose, the first three processing stages depicted in Fig. 4 are separately applied at the K receiving channels and the complex values obtained for a given range-angle bin are collected in the K-dimensional vector $\boldsymbol{x}$:

$$\boldsymbol{x}\ [l,p] = [\zeta_0\,[l,p]\,,\ \zeta_1\,[l,p]\,,\ \ldots,\ \zeta_{K-1}\,[l,p]]^T \tag{8}$$

where the superscript T denotes the transpose operation. We recall that $\boldsymbol{x}\ [l,p] = \boldsymbol{x}[l,-p]$ due to the ambiguous mapping of Doppler frequencies into azimuth angles.

The removal of the left/right ambiguity is sought by spatial filtering, namely by applying an angle-bin dependent digital beamforming to the available receiving channels. Specifically, for each angle (Doppler) bin, the beam is steered towards the corresponding direction $\varphi_0 = \varphi[p]$, while the returns from the ambiguous direction $-\varphi_0 = \varphi[-p]$, are suppressed. This allows to obtain a final range-angle map where the left-right ambiguities are largely mitigated:

$$\eta\ [l,p] = \boldsymbol{w}^H\,[p]\,\boldsymbol{x}\,[l,p] \tag{9}$$

where H denotes the Hermitian transpose operation.

The effectiveness of the ambiguity removal depends on the employed spatial filtering strategy. The easiest approach is to

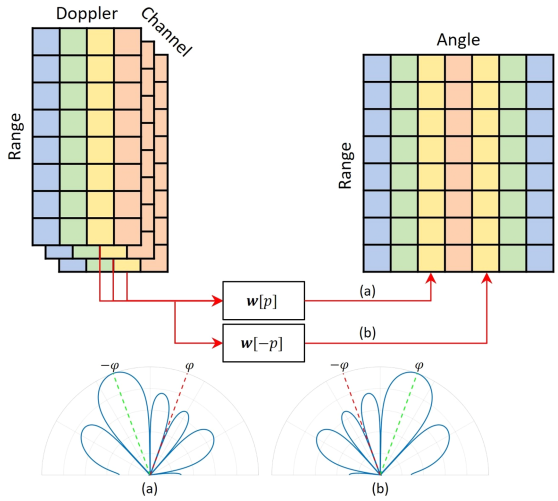

Fig. 7. Sketch of the proposed algorithm for range-angle map evaluation and left/right ambiguity resolution.

just steer the beam in the desired directions, relying only on the spatial selectivity of the array beam pattern:

$$\boldsymbol{w}_{steer} = \boldsymbol{s}/\|\boldsymbol{s}\|^2 \tag{10}$$

where $\mathbf{s}$ is the steering vector evaluated for the direction φ associated to the Doppler frequency f_D. Specifically, assuming a linear array of K antennas arranged parallel to the y-axis, it can be expressed as

$$\begin{aligned}\boldsymbol{s}\ (\varphi) &= \left[1, e^{j\frac{2\pi}{\lambda}\ d_1 \sin\varphi}, \ldots, e^{j\frac{2\pi}{\lambda}\ d_{K-1}\sin\varphi}\right]^T \\ &= \left[1, e^{j\frac{2\pi}{\lambda}\ d_1\sqrt{1-(f_D\lambda/v_p)^2}}, \ldots, e^{j\frac{2\pi}{\lambda}\ d_{K-1}\sqrt{1-(f_D\lambda/v_p)^2}}\right]^T\end{aligned} \tag{11}$$

where d_i denotes the distance of the i-th array element with respect to the first one, assumed as a reference without loss of generality. Note that the steering vector in the corresponding ambiguous direction is $\boldsymbol{s}\ (-\varphi) = \bar{\boldsymbol{s}}\ (\varphi)$.

The approach above is expected to mitigate only partially the angular ambiguity issue. In fact, due to the typical restrictions of passive radar in terms of compactness and cost of the system, and to the low carrier frequencies of common illuminators of opportunity, a limited number of receiving channels is generally available, resulting in array patterns with relatively large beams. This is in turn provides a quite poor angular discrimination capability that will be shown to be inadequate to effectively resolve the left/right ambiguity.

Therefore, in this study, a spatial filtering algorithm based on digital beamforming and array-based directional nulling techniques is proposed as a more suitable solution.

Fig. 7 shows a sketch of the proposed algorithm for the formation of the range-angle map by DBS and for the removal of the left/right ambiguity by spatial filtering. The operations illustrated correspond to the last two blocks of the processing scheme reported in Fig. 4.

It is worth recalling that, in the considered scheme, the angular resolution is derived from the Doppler resolution via DBS, while the spatial beamforming only operates on the removal of the left/right ambiguity.

Several possible strategies are available for the spatial filtering, aimed at maximising the response in one direction, while suppressing the other potential undesired contributions. Among these, the minimum variance distortion-less response (MVDR) beamformer is probably the most straightforward, [36]. As known, it minimizes the array output power while setting the gain in the desired direction to unity. The MVDR beamformer weights are given by

$$\boldsymbol{w}_{MVDR} = \boldsymbol{R}^{-1}\ \boldsymbol{s}/\left(\boldsymbol{s}^H\boldsymbol{R}^{-1}\boldsymbol{s}\right) \tag{12}$$

where $\boldsymbol{R}$ represents the disturbance covariance matrix. In our case, the disturbance covariance matrix can be set as $\boldsymbol{R} = r(\bar{\boldsymbol{s}}\bar{\boldsymbol{s}}^H) + \boldsymbol{I}$, so as to model an undesired signal in the ambiguous direction, where r defines its power level above noise, and $\boldsymbol{I}$ denotes the identity matrix.

An alternative approach can be to constrain the array response in the desired direction to unity and in the ambiguous direction to be less than a defined value q, while minimising the norm of the weight vector, namely the output noise power. This corresponds to solve the following convex optimization (CO) problem, and it will be referred to as CO approach

$$\begin{aligned}\boldsymbol{w}_{CO}\ :\ &\min\ \|\boldsymbol{w}\| \\ &\text{s.t. } \boldsymbol{w}^H\boldsymbol{s} = 1 \\ &\left|\boldsymbol{w}^H\bar{\boldsymbol{s}}\right| < q\end{aligned} \tag{13}$$

To analyse and compare the effectiveness of the proposed approaches, we consider two performance parameters, which encode the obtained increase in SNR values and the residual ambiguity level. Specifically, we introduce the SNR improvement I_{SNR} and the Doppler-ambiguity ratio (DAR) improvement I_{DAR}, defined as the ratio of the SNR values and of the DAR values, respectively, at the input and at the output of the spatial beamformer:

$$\begin{aligned}I_{SNR} &= \frac{SNR_{out}}{SNR_{in}} = \frac{\left|\boldsymbol{w}^H\boldsymbol{s}\right|^2}{\boldsymbol{w}^H\boldsymbol{w}} \\ I_{DAR} &= \frac{DAR_{out}}{DAR_{in}} = \frac{\left|\boldsymbol{w}^H\boldsymbol{s}\right|^2}{\left|\boldsymbol{w}^H\bar{\boldsymbol{s}}\right|^2}\end{aligned} \tag{14}$$

Fig. 8 shows the expected performance of the proposed left/right ambiguity resolution strategy, assuming an ULA of $K = 3$ elements spaced by $\lambda/2$ from each other. The results are given in terms of the introduced parameters, as functions of the steering direction. The MVDR beamformer (solid curves) was applied with $r = 100$. The CO approach (dashed curves) was applied with $q = 0.001$. The values of r and q were empirically selected so as the two approaches provided comparable level of ambiguity removal.

For comparison, Fig. 8 also includes the corresponding performance obtained with a simple beam steering approach, as from (10), which only steers the array beam in the desired directions, without pattern nulling (dash-dotted curves).

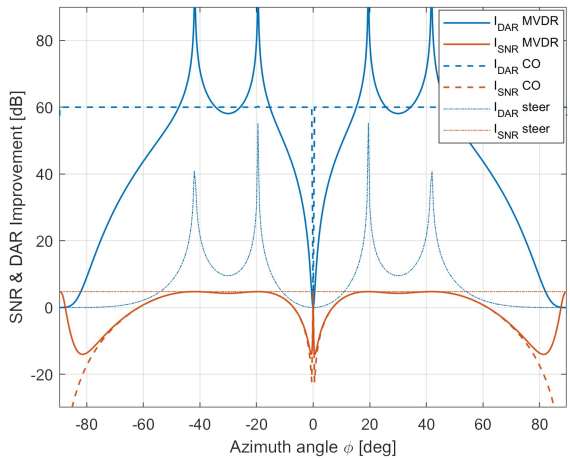

Fig. 8. Left/right ambiguity resolution performance as a function of the steering angle, assuming an ULA of three element with $\lambda/2$ spacing. MVDR and CO beamformers provide effective ambiguity removal, although a wide notch is still present for angles close to the forward-looking direction.

As apparent, due to the limited number of channels typical of passive radar, the simple spatial selectivity of array beam steering proves inadequate to effectively resolve the left/right ambiguity, resulting in poor overall I_{DAR} performance.

On the other hand, both the proposed approaches allow to significantly attenuate the ambiguous contributions, while preserving the useful signal. The MVDR beamformer tends to bring the ambiguity output power to the noise level and to provide the best signal to disturbance ratio, while the CO approach ensures to attenuate the ambiguous contribution up to the fixed desired level, regardless of the effect on the SNR.

Notice that a relatively wide performance notch is still present for angles close to the forward-looking direction (i.e., $\varphi = 0°$). This is due to the proximity of the two ambiguous directions φ and $-\varphi$, namely the direction of interest and the desired pattern nulling, which makes it difficult to suppress the ambiguity and simultaneously preserve the useful signal. In the MVDR case, this is clearly visible on both the SNR and DAR improvement. In the CO case, although the interference removal is effective, it sensibly affects the SNR improvement.

To improve the effectiveness of the left/right ambiguity resolution at angles close to the forward-looking direction, a sufficiently narrow antenna beamwidth would be required, thus defining a constraint on the minimum size of the array.

B. Array Design Considerations

In general, potential constraints on the array size might derive from system design and implementation aspects. For instance, a minimum antenna gain would be required for the receiving system to capture also weak signals. This may determine a minimum size for the array and, in the case of few available receiving channels, it may impose some restrictions on the physical displacement of the antenna elements connected to those channels, based on their specifications and practical implementation.

While the constraints above depend on the specific implementation, we want to address the restrictions that come from the angular resolution constraints. We recall that, in the proposed system, the azimuth resolution is obtained from the Doppler frequency resolution via a DBS technique. However, as mentioned, a small width for the resulting array beam may still be required to guarantee an effective left/right ambiguity removal also at angles close to the forward-looking direction.

A larger array size would allow to shrink the performance notch. Ideally, this notch is desired to be sufficiently narrow to enable an effective resolution of the ambiguity up to a minimum angle of interest, compatible with the expected angular resolution around 0°, which in turn depends on the platform velocity and the integration time.

This can be obtained by imposing the array beamwidth to be smaller than the minimum expected distance between the direction of interest and the corresponding ambiguous one. By calling L_a the length of the array and φ_{min} the minimum angle of interest, the above can be approximately expressed as

$$\frac{\lambda}{L_a \cos\varphi_{min}} < 2\varphi_{min} \tag{15}$$

Considering the Doppler resolution $\delta\ f_D = 1/T_i$, the angle φ_{min} might be assumed as the angle corresponding to the Doppler frequency bin $f_D^{max} - \delta\ f_D = v_p\ /\lambda - 1/T_i$, that is

$$\varphi_{min} = \arccos\left[\left(\frac{v_p}{\lambda} - \frac{1}{T_i}\right)\frac{\lambda}{v_p}\right] = \arccos\left(1 - \frac{\lambda}{v_p T_i}\right) \tag{16}$$

where it was implicitly assumed that $T_i > \lambda/v_p$. As a result, the condition in (15) can be expressed as

$$L_a > \frac{\lambda}{2\left(1 - \frac{\lambda}{v_p T_i}\right)\arccos\left(1 - \frac{\lambda}{v_p T_i}\right)} \tag{17}$$

Notice that the required array length increases when the platform velocity and/or the integration time increase. The above constraint leads to a minimum requirement on the size of the array. However, in the case of few available receiving channels, this may result in the presence of grating lobes in the final array pattern, due to the resultant spatial undersampling, which might cause considerable performance degradation in the ambiguity resolution process.

Fig. 9(a) shows the expected performance for the case of a ULA of $K = 3$ elements spaced by $5\lambda/4$ from each other. Assuming the same system parameters of Table I, for the case of a DVB-S illuminator, this corresponds to an array length $L_a = 5\lambda/2 \cong 6.8\ cm$, which meets the condition in (17). As evident, the larger array length allows to shrink the central performance notch, compared to results in Fig. 8, providing good ambiguity attenuation up to angles close to the forward-looking direction, and comparable with the expected angular resolution capability. However, additional notches appear due to the presence of grating lobes in the resulting array pattern.

To solve this problem, while keeping low the number of receiving channels, and so the complexity of the receiver, we can resort to non-uniform distributions of antennas. Fig. 9(b) reports the ambiguity resolution performance assuming a NULA of $K = 3$ antennas with an inter-element spacing $[0, \lambda, 5\lambda/2]$.

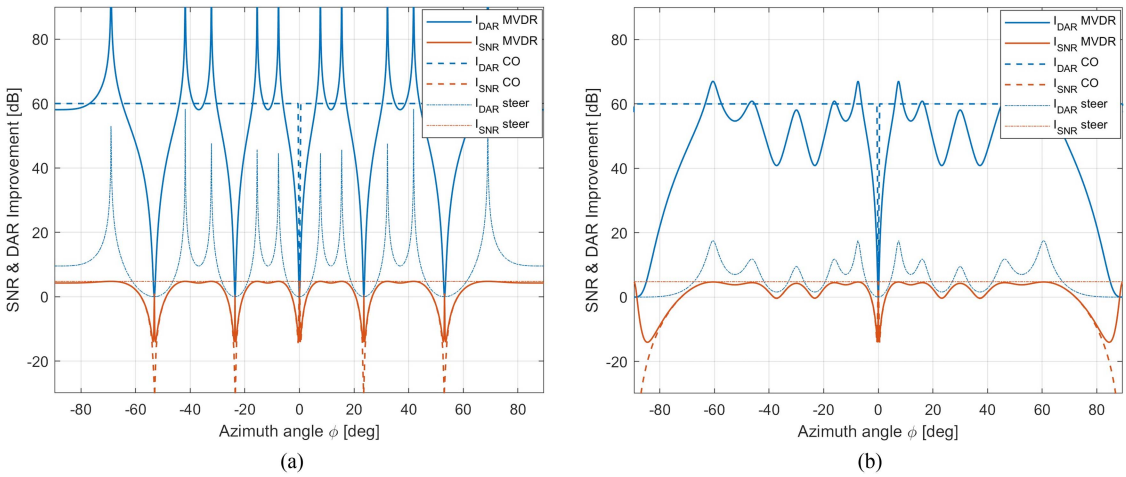

Fig. 9. Left/right ambiguity resolution performance assuming an array of three elements with length $5\boldsymbol{\lambda}/2$: (a) ULA $[0,\ 5\boldsymbol{\lambda}/4,\ 5\boldsymbol{\lambda}/2]$; (b) NULA $[0, \boldsymbol{\lambda}, 5\boldsymbol{\lambda}/2]$. The array length was selected according to the criterion in (17). Effective ambiguity removal is achieved up to angles close to the forward-looking direction and comparable with the expected angular resolution. The NULA configuration prevents the appearance of additional undesired notches due to grating lobes.

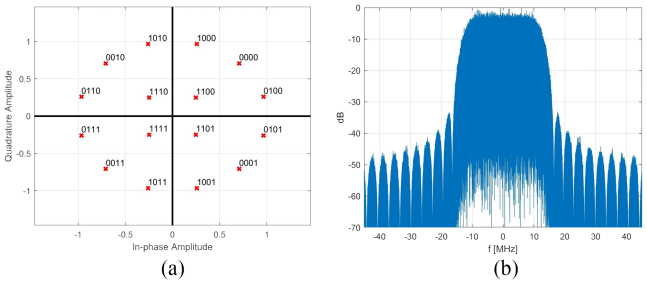

Fig. 10. Simulated reference signal according to the DVB-S2 standard: (a) 16APSK constellation; (b) signal power spectrum.

This specific NULA configuration was selected according to the design strategy proposed in [37], where a half-wavelength quantization of the inter-element spacing is considered. Moreover, this array configuration has the same total length of the previous ULA case. Compared to ULA, the selected NULA configuration provides the same advantages for angles close to $\varphi = 0°$, but it prevents the significant performance losses due to the grating lobes, at the expense of some residual fluctuations. Again, this effect is clearly visible on both the DAR and SNR improvement for the MVDR beamformer, while it can be only appreciated on the SNR performance for the CO case.

Note that, if longer arrays were considered, i.e., beyond the criterion in (17), the performance notch would be narrower than necessary, ideally enabling effective ambiguity removal for directions below the minimum discriminable angle of interest. Moreover, it would worsen the residual performance fluctuations, unless more receiving channels were available.

C. Apodization Technique

By applying the above spatial filtering strategies for the removal of the left/right ambiguity with a properly designed array configuration, the scatterers in all the angular sector of interest of the observed area can be associated to their correct angular position. Namely, the echoes arriving from the left and right angular sectors can be separated and distinguished.

The presence of some residual fluctuations in the SNR performance, such as those seen in Fig. 9(b), may produce an undesirable increase of the noise level in the final range-angle map, in correspondence of some specific directions, according to the adopted array configuration. Specifically, the position of the null may unnecessarily increase the noise even where there is no significant ambiguous contribution to be removed.

To mitigate this problem and further improve the final SNR performance, an apodization strategy is introduced.

According to this strategy, the final map obtained through the MVDR or CO beamformer described above is combined with the map provided by a simple beamformer, which only steers the array beam alternately on the two angular directions associated to each Doppler bin. Note that a simple beam steering allows us to maximise the final SNR but does not suppress the potential ambiguous contribution.

The two maps are combined by taking the minimum for each pixel, according to the following

$$y = \min\left(\left|\boldsymbol{w}_{\gamma}^{H}\boldsymbol{x}\right|, \left|\boldsymbol{w}_{steer}^{H}\boldsymbol{x}\right|\right) \tag{18}$$

where the beamformer weights $\boldsymbol{w}_{\gamma}$ are selected according to the MVDR or CO solution. In principle, this approach would preserve the cancellation of the ambiguities, while preventing the unwanted increase of the noise level, especially in those regions where no significant contributions need to be cancelled in the corresponding ambiguous direction.

An evaluation of the effect of the described apodization strategy and, more in general, of the effectiveness of the proposed left/right ambiguity resolution scheme is addressed in the next section, against simulated data.

IV. Simulated Results

A simulated scenario was generated in order to validate the capabilities of the system in a controlled environment. A radar

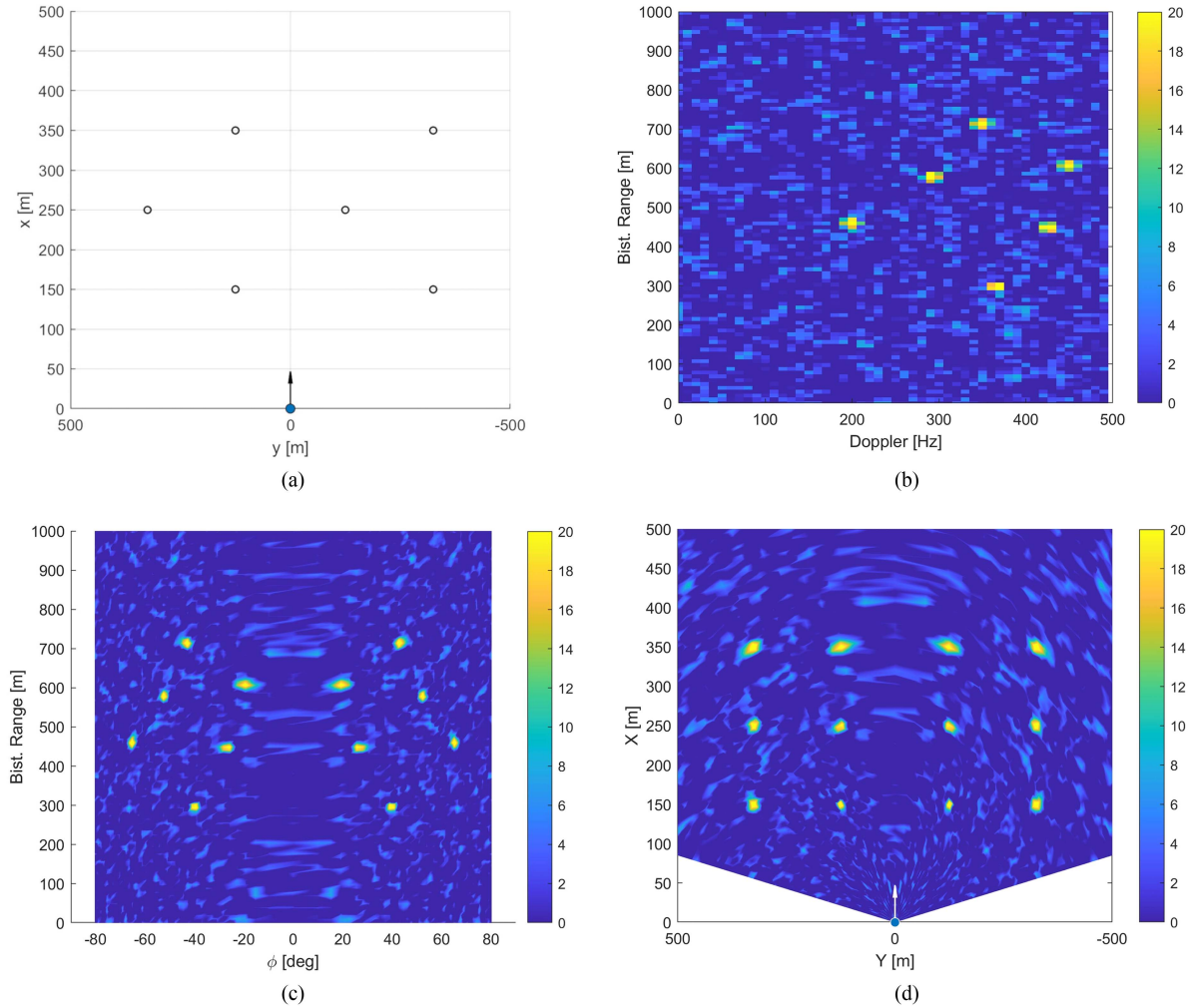

Fig. 11. Simulated scenario and results of single channel processing: (a) Position of the simulated scatterers (black circles) with respect to position and direction of motion of the receiver (blue filled circle); (b) range-doppler map obtained at single channel; (c) range-angle map obtained by rescaling the doppler axis into azimuth angle according to DBS; (d) corresponding cartesian plot showing scatterers in both real and ambiguous positions.

equipped with $K = 3$ surveillance channels was assumed, installed on a ground moving vehicle in a forward-looking configuration and exploiting the signal transmitted by a geostationary satellite illuminator. The area of interest was supposed to be a front angular sector spanning [-80°,80°]. The same system parameters and bistatic geometry considered in Section II were assumed. The reference signal was generated according to the DVB-S2 downlink standard [38], assuming a 16APSK modulation and a signal bandwidth of approximately 30 MHz (see Fig. 10).

The scenario consists of six ground fixed scatterers located in the vicinity of the receiver and positioned as shown in Fig. 11(a). Their echo signal was generated as a superposition of delayed and Doppler shifted replicas of the reference signal. The received surveillance signal includes the echo signal and thermal noise, with an arbitrarily set SNR level.

Fig. 11(b) shows the range-Doppler map obtained at single channel, at the output of the sub-optimal batch implementation of (3). The six fixed scatterers are well focused and spaced in Doppler frequency according to their angular directions. Note that a 30 dB Taylor tapering window was applied both in range and Doppler to help reducing the sidelobe level.

In Fig. 11(c), by assuming a known receiver velocity and following the DBS approach, the Doppler frequency axis was mapped into the azimuth angle axis according to (2). Finally, in Fig. 11(d), based on the knowledge of both the receiver and transmitter position, the observed data were mapped into their Cartesian x-y coordinates, delivering a simple localization of the scatterers with respect to the vehicle.

As expected, due to the cited left/right ambiguity problem, when operating with a single channel, the radar is not able to discriminate from which of the two ambiguous directions associated with each Doppler bin a given scatterer comes from. As a result, the map in Fig. 11(c) and (d) is characterized by the presence of ambiguous replicas of the scatterers, easily identifiable from a comparison with Fig. 11(a).

To overcome this problem, the multichannel processing algorithm proposed in Section III was applied, assuming a NULA of $K = 3$ elements spaced by $[0, \lambda, 5\lambda/2]$ along the y-axis. This configuration corresponds to that considered in Section III,

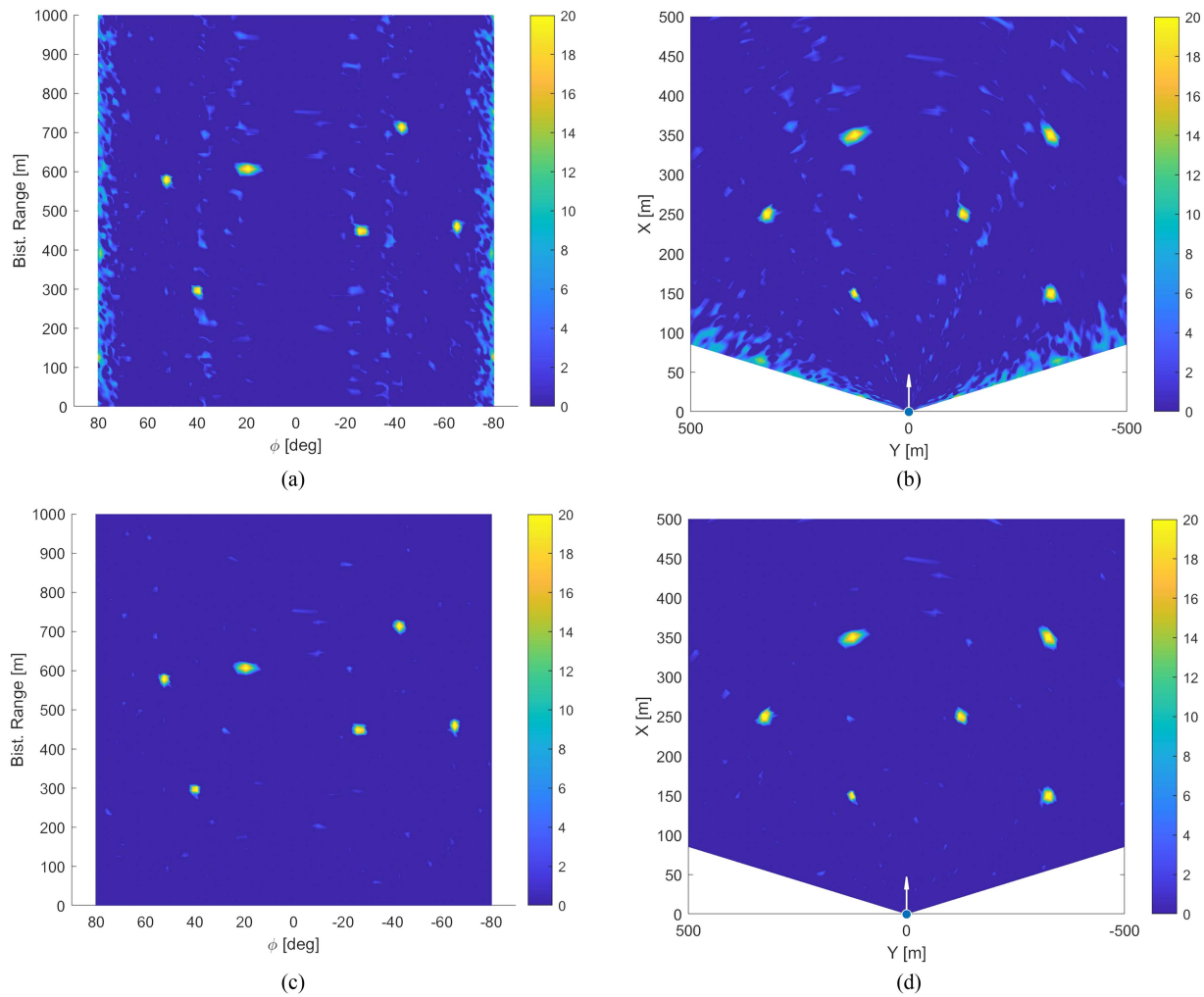

Fig. 12. Results of multichannel processing: (a) and (b) range-angle map and Cartesian plot obtained after left/right ambiguity removal; (c) and (d) range-angle map and Cartesian plot obtained after ambiguity removal and apodization. All the scatterers are correctly localized with respect to the receiver position.

whose theoretical performance is reported in Fig. 9(b). Specifically, the MVDR beamformer was employed. The range-angle map and the corresponding Cartesian plot obtained at the output of the ambiguity resolution algorithm, are reported in Fig. 12(a) and (b), respectively.

Thanks to the adopted spatial filtering and the appropriate array configuration, all the scatterers were correctly associated to their angular direction and their ambiguous replicas were removed from the map. From a comparison with Fig. 11(a), the remaining scatterers have been properly positioned.

As expected, a slight variation in the achieved resolution can be appreciated, according to the position of the scatterer. In particular, the resolution in azimuth degrades as the range increase and getting closer to the forward-looking direction. Moreover, an improvement of the SNR level can be noticed, given by the coherent combination of the K channels. This is expected to be in the order of 4.7 dB. Anyway, due to the SNR performance fluctuations seen in Fig. 9(b), a higher level of noise is present in correspondence of some specific directions. Note that the gain on target of the beamformer is set to unity.

To mitigate this issue and improve the SNR performance in the final map, the proposed apodization strategy was applied. Specifically, the map shown in Fig. 12(a) and (b) was combined with that obtained at the output of a simple beamformer, according to (12). The result is reported in Fig. 12(c) and (d). As expected, this approach was able to preserve the cancellation of the ambiguous scatterers, while preventing the undesirable fluctuations in the noise level, especially in those regions where no significant ambiguities needed to be cancelled. This ultimately provides a cleaner version of the final map, potentially facilitating a subsequent detection stage.

It is worth noting that the proposed approach is expected to operate effectively also in the presence of numerous scatterers, with obvious limitations when the level of the corresponding echoes shows a high dynamic range. However, even in this case, the relevant parameters of the proposed algorithms can be adjusted to improve the rejection of the ambiguity at the expense of the SNR.

To complete the analysis, Fig. 13(a) illustrates the corresponding map in Cartesian coordinates obtained using a simple beam steering approach, with no pattern nulling, as in (10).

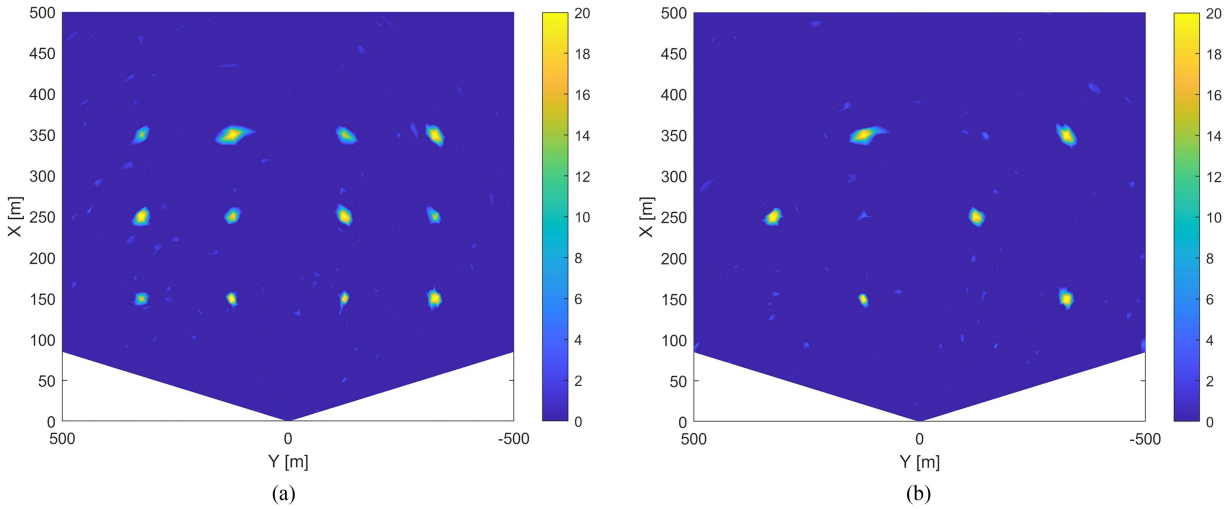

Fig. 13. Cartesian plots obtained after: (a) Simple beam steering approach with no pattern nulling; (b) ambiguity removal with CO approach and apodization.

As expected, the limited number of receiving channels and the relatively large beam (approximately 23°), make the spatial selectivity of array steering insufficient to resolve the left/right ambiguity, producing just a minor attenuation of the ambiguous replicas of the scatterers, whose level depends on their positioning with respect to the sidelobes of the pattern.

In addition, Fig. 13(b) reports the Cartesian plot obtained after ambiguity removal and apodization, when using the CO beamformer approach. By a comparison with Fig. 12(c), this confirms that the proposed MVDR and CO beamformers offer similar results, if appropriate parameters are selected to guarantee a sufficiently high DAR improvement level.

Finally, it is worth recalling that this system concept relies on the radar motion to refine the angular resolution in azimuth and discriminate the fixed scatterers across the antenna beam. As a result, potential moving targets would appear misplaced in the final map due to their own radial velocity component. Although not the focus of this article, the presence of moving targets, as well as the impact of range and Doppler migrations within the CPI, are likely to be common in the automotive scenario. Addressing these issues requires the implementation of strategies for motion compensation, image focusing, and moving target indication, which are well known in the active radar literature and will be the subject of future studies.

V. Conclusion

This article investigated the potential use of a passive radar sensor onboard a vehicle to enable automotive applications based on the exploitation of an external illumination source. This concept would enable the coexistence of different radar systems sharing the same transmitted signal, removing the problem of mutual interference in congested environments.

The possible external illuminators include third-party noncooperative transmitters, such as broadcast communication systems, as well as dedicated signals emitted by upcoming vehicle to infrastructure connection systems. In this work, a geostationary satellite DVB-S transmitter has been primarily considered as an illuminator of opportunity.

Although some simplifying hypotheses were assumed, the preliminary analysis showed reasonable performance in terms of coverage and spatial resolution, even operating with a single transmitter and a relatively short integration times, and despite the large distance of the selected illuminator.

The possibility to discriminate stationary scatterers in the vicinity of the vehicle, both in range and azimuth directions, and to correctly locate them with respect to the receiver position was showed by exploiting an efficient DBS approach.

The problem of left/right Doppler ambiguity arising from the forward-looking observation geometry was addressed, by exploiting multichannel processing. An ambiguity removal algorithm was proposed, based on MVDR or CO digital beamformers, which allows to steer the beam in the desired direction, while suppressing the echoes from the ambiguous one, thus enabling the formation of an unambiguous range-Doppler map via DBS.

Moreover, some criteria for the design of the array with a limited number of elements were derived, suggesting the use of NULA configurations to improve the effectiveness of the ambiguity removal for angles close to the motion direction, while preventing significant performance losses due to grating lobes. In addition, undesirable fluctuations of the final noise level were prevented, resorting to an apodization strategy.

Finally, the effectiveness of the proposed solutions was verified in a simulated scenario, where they provided the correct mapping of all the scatterers in the observed scene.

Although the coverage and spatial resolution performance achievable in the considered case study may not be up to the standard typically required for automotive applications, they may still offer useful information for the safety of the vehicle. Notice that the proposed system concept might be intended as a secondary/backup solution to rely on in the case of a highly congested environment. Such promising results evidence the potentiality of a receive-only solution for automotive radar applications and suggest the need for further studies.

Future research will focus on investigating algorithmic and architectural solutions to further improve the achievable performance and reliability of the system and to deal with the presence of moving targets and possible migration effects. Moreover, solutions exploiting alternative transmitters and waveforms of opportunity will be explored.

REFERENCES

[1] J. Hasch, E. Topak, R. Schnabel, T. Zwick, R. Weigel, and C. Waldschmidt, "Millimeter-wave technology for automotive radar sensors in the 77 GHz frequency band," *IEEE Trans. Microw. Theory Techn.*, vol. 60, no. 3, pp. 845–860, Mar. 2012.

[2] A. John and T. Schipper, "More safety for all by radar interference mitigation D5.4–Conclusion and outlook how to solve still open challenges," Eur. Commission, Brussels, Belgium, Report MOSARIM No. 248231, 2012.

[3] W. Buller et al., "Radar congestion study," Nat. Highway Traffic Saf. Admin., Washington, DC, USA, Tech. Rep. DOT HS 812 632, 2018.

[4] A. Bourdoux, K. Parashar, and M. Bauduin, "Phenomenology of mutual interference of FMCW and PMCW automotive radars," in *Proc. IEEE Radar Conf.*, 2017, pp. 1709–1714.

[5] F. Uysal and S. Sanka, "Mitigation of automotive radar interference," in *Proc. IEEE Radar Conf.*, 2018, pp. 0405–0410.

[6] M. Toth, J. Rock, P. Meissner, A. Melzer, and K. Witrisal, "Analysis of automotive radar interference mitigation for real-world environments," in *Proc. IEEE 17th Eur. Radar Conf.*, 2021, pp. 176–179.

[7] S. Neemat, O. Krasnov, and A. Yarovoy, "An interference mitigation technique for FMCW radar using beat-frequencies interpolation in the STFT domain," *IEEE Trans. Microw. Theory Techn.*, vol. 67, no. 3, pp. 1207–1220, Mar. 2019.

[8] M. Umehira, T. Okuda, X. Wang, S. Takeda, and H. Kuroda, "An adaptive interference detection and suppression scheme using iterative processing for automotive FMCW radars," in *Proc. IEEE Radar Conf.*, 2020, pp. 1–5.

[9] S. Chen, J. Taghia, U. Kühnau, T. Fei, F. Grünhaupt, and R. Martin, "Automotive radar interference reduction based on sparse Bayesian learning," in *Proc. IEEE Radar Conf.*, 2020, pp. 1–6.

[10] G. K. Carvajal et al., "Comparison of automotive FMCW and OFDM radar under interference," in *Proc. IEEE Radar Conf.*, 2020, pp. 1–6.

[11] F. Uysal, "Phase-coded FMCW automotive radar: System design and interference mitigation," *IEEE Trans. Veh. Technol.*, vol. 69, no. 1, pp. 270–281, Jan. 2020.

[12] Y. L. Sit, B. Nuss, and T. Zwick, "On mutual interference cancellation in a MIMO OFDM multiuser radar-communication network," *IEEE Trans. Veh. Technol.*, vol. 67, no. 4, pp. 3339–3348, Apr. 2018.

[13] F. Norouzian, A. Pirkani, E. Hoare, M. Cherniakov, and M. Gashinova, "Automotive radar waveform parameters randomisation for interference level reduction," in *Proc. IEEE Radar Conf.*, 2020, pp. 1–5.

[14] G. Hakobyan, K. Armanious, and B. Yang, "Interference-aware cognitive radar: A remedy to the automotive interference problem," *IEEE Trans. Aerosp. Electron. Syst.*, vol. 56, no. 3, pp. 2326–2339, Jun. 2020.

[15] K. U. Mazher, R. W. Heath, K. Gulati, and J. Li, "Automotive radar interference characterization and reduction by partial coordination," in *Proc. IEEE Radar Conf.*, 2020, pp. 1–6.

[16] J. Choi, V. Va, N. Gonzalez-Prelcic, R. Daniels, C. R. Bhat, and R. W. Heath, "Millimeter-wave vehicular communication to support massive automotive sensing," *IEEE Commun. Mag.*, vol. 54, no. 12, pp. 160–167, Dec. 2016.

[17] P. Kumari, J. Choi, N. González-Prelcic, and R. W. Heath, "IEEE 802.11ad-based radar: An approach to joint vehicular communication-radar system," *IEEE Trans. Veh. Technol.*, vol. 67, no. 4, pp. 3012–3027, Apr. 2018.

[18] R. S. Thoma et al., "Cooperative passive coherent location: A promising 5G service to support road safety," *IEEE Commun. Mag.*, vol. 57, no. 9, pp. 86–92, Sep. 2019.

[19] A. Ali, N. González-Prelcic, and A. Ghosh, "Passive radar at the roadside unit to configure millimeter wave vehicle-to-infrastructure links," *IEEE Trans. Veh. Technol.*, vol. 69, no. 12, pp. 14903–14917, Dec. 2020.

[20] B. Dawidowicz, K. S. Kulpa, M. Malanowski, J. Misiurewicz, P. Samczynski, and M. Smolarczyk, "DPCA detection of moving targets in airborne passive radar," *IEEE Trans. Aerosp. Electron. Syst.*, vol. 48, no. 2, pp. 1347–1357, Apr. 2012.

[21] P. Wojaczek, F. Colone, D. Cristallini, and P. Lombardo, "Reciprocal filter-based STAP for passive radar on moving platforms," *IEEE Trans. Aerosp. Electron. Syst.*, vol. 55, no. 2, pp. 967–988, Apr. 2019.

[22] G. P. Blasone, F. Colone, P. Lombardo, P. Wojaczek, and D. Cristallini, "Passive radar DPCA schemes with adaptive channel calibration," *IEEE Trans. Aerosp. Electron. Syst.*, vol. 56, no. 5, pp. 4014–4034, Oct. 2020.

[23] G. P. Blasone, F. Colone, P. Lombardo, P. Wojaczek, and D. Cristallini, "Passive radar STAP detection and DOA estimation under antenna calibration errors," *IEEE Trans. Aerosp. Electron. Syst.*, vol. 57, no. 5, pp. 2725–2742, Oct. 2021.

[24] D. Gromek, K. Kulpa, and P. Samczyński, "Experimental results of passive SAR imaging using DVB-T illuminators of opportunity," *IEEE Geosci. Remote Sens. Lett.*, vol. 13, no. 8, pp. 1124–1128, Aug. 2016.

[25] Y. Fang et al., "Improved passive SAR imaging with DVB-T transmissions," *IEEE Trans. Geosci. Remote Sens.*, vol. 58, no. 7, pp. 5066–5076, Jul. 2020.

[26] G. P. Blasone, F. Colone, and P. Lombardo, "Passive radar concept for automotive applications," in *Proc. IEEE Radar Conf.*, 2022, pp. 1–5.

[27] J. Rosado-Sanz, M. P. Jarabo-Amores, D. Mata-Moya, N. del-Rey-Maestre, and A. Almodovar-Hernandez, "DVB-S Passive radar performance evaluation in semi-urban ground scenario," in *Proc. IEEE 21st Int. Radar Symp.*, 2020, pp. 232–235.

[28] T. Martelli, O. Cabrera, F. Colone, and P. Lombardo, "Exploitation of long coherent integration times to improve drone detection in DVB-S based passive radar," in *Proc. IEEE Radar Conf.*, 2020, pp. 1–6.

[29] F. Filippini, O. Cabrera, C. Bongioanni, F. Colone, and P. Lombardo, "DVB-S based passive radar for short range security application," in *Proc. IEEE Radar Conf.*, 2021, pp. 1–6.

[30] J. Li et al., "A DVB-S-based multichannel passive radar system for vehicle detection," *IEEE Access*, vol. 9, pp. 2900–2912, 2021.

[31] F. Colone, D. W. O'Hagan, P. Lombardo, and C. J. Baker, "A multistage processing algorithm for disturbance removal and target detection in passive bistatic radar," *IEEE Trans. Aerosp. Electron. Syst.*, vol. 45, no. 2, pp. 698–722, Apr. 2009.

[32] P. Lombardo and F. Colone, "Advanced processing methods for passive bistatic radar systems," in *Principles of Modern Radar: Advanced Radar Techniques*, Raleigh, NC, USA: SciTech Publishing, 2012, pp. 739–821.

[33] P. Samczyński et al., "5G network-based passive radar," *IEEE Trans. Geosci. Remote Sens.*, vol. 60, 2022, Art. no. 5108209.

[34] G. P. Cardillo, "On the use of the gradient to determine bistatic SAR resolution," in *Proc. IEEE Int. Symp. Antennas Propag. Soc., Merging Technol. 90's*, 1990, pp. 1032–1035.

[35] C. A. Wiley, "Synthetic aperture radars," *IEEE Trans. Aerosp. Electron. Syst.*, vol. AES-21, no. 3, pp. 440–443, May 1985.

[36] H. L. Van Trees, *Optimum Array Processing, (Detection, Estimation, and Modulation Theory, Part IV)*, Hoboken, NJ, USA: Wiley, 2002.

[37] R. L. Goodwin, "Ambiguity-resistant three-and four-channel interferometers," Naval Res. Lab., WA, DC, USA, NRL Rep. 8005, 1976.

[38] Digital Video Broadcasting (DVB): Second generation framing structure, channel coding and modulation systems for broadcasting, interactive services, news gathering and other broadband satellite applications; European Telecommunications Standards Institute (ETSI), EN 302 307-1, 650 Route des Lucioles F-06921 Sophia Antipolis Cedex, France, 2014.

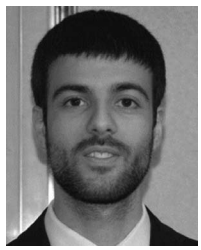

Giovanni Paolo Blasone (Member, IEEE) received the M.Sc. degree (with Hons.) in telecommunication engineering and the Ph.D. degree (with Hons.) in radar and remote sensing from the Sapienza University of Rome, Rome, Italy, in 2016 and 2021, respectively. Since 2021, he has been a Postdoctoral Researcher with the Department of Information Engineering, Electronics and Telecommunications, Sapienza University of Rome. His main research interests include adaptive signal processing for multichannel radar systems and passive radar GMTI. He has been involved in research projects funded by the Italian Space Agency, Italian Ministry of Research, and national radar industry. He was the Finalist in the Student Paper Competition at the 2020 IEEE International Radar Conference, in the 3MT Contest at the 2020 IEEE Radar Conference and in the 2021 GTTI PhD Award.

Fabiola Colone (Senior Member, IEEE) received the Degree in telecommunications engineering and the Ph.D. degree in remote sensing from the Sapienza University of Rome, Rome, Italy, in 2002 and 2006, respectively. In January 2006, she joined the DIET Department, Sapienza University of Rome, as a Research Associate. From December 2006 to June 2007, she was a Visiting Scientist with the Electronic and Electrical Engineering Department, University College London, London, U.K. She is currently a Full Professor with the Faculty of Information Engineering, Informatics, and Statistics, Sapienza University of Rome, where she is also the Chair of the degree programs in communications engineering. The majority of her research activity is devoted to radar systems and signal processing. She has been involved, with scientific responsibility roles, in research projects funded by the European Commission, European Defence Agency, Italian Space Agency, Italian Ministry of Research, and many radar/ICT companies. Her research has been reported in more than 160 publications in international technical journals, book chapters, and conference proceedings. She is the co-editor of the book *Radar Countermeasures for Unmanned Aerial Vehicles*, IET Publisher. She was the co-recipient of the 2018 Premium Award for Best Paper in IET Radar, Sonar & Navigation. From 2017 to 2022, she was a Member of the Board of Governors of the IEEE Aerospace and Electronic System Society (AESS) in which she was the Vice-President for Member Services, and Editor in Chief for the IEEE AESS QEB Newsletters. She is an IEEE Senior Member since 2017, and a Member of the IEEE AESS Radar System Panel since 2019. Dr. Colone is an Associate Editor in Chief for the IEEE TRANSACTIONS ON RADAR SYSTEMS. From 2017 to 2020, she was an Associate Editor for the IEEE TRANSACTIONS ON SIGNAL PROCESSING. She is a Member of the Editorial Board of the *International Journal of Electronics and Communications* (Elsevier). She was with the organizing committee and technical program committee of many international conferences. She was the Technical Co-Chair of the IEEE 2021 Radar Conference (Atlanta, USA) and European Radar Conference EuRAD 2022 (Milan, Italy).

Pierfrancesco Lombardo (Senior Member, IEEE) received the Degree in electronic engineering and the Ph.D. degree in remote sensing from the University of Rome La Sapienza, Rome, Italy, in 1991 and 1995, respectively.

After serving on the Official Test Centre of the Italian Air Force in 1992, he was an Associate with Birmingham University, Birmingham, U.K., and Defence Research Agency in Malvern, in 1994. In 1995, he was a Research Associate with Syracuse University, Syracuse, NY, USA. In 1996, he joined the University of Rome La Sapienza, where he is currently a Full Professor. He is involved in, and coordinates, research projects funded by European and National Research Agencies and national industries. He leads the Radar, Remote Sensing and Navigation Group, University of Rome La Sapienza. His main research interests include radar adaptive signal processing, radar clutter modelling, radar coherent detection, passive radar and multistatic radar, SAR processing, and radio-localization systems. His research has been reported in more than 320 publications in international technical journals and conferences a book and seven book chapters. Dr. Lombardo was the co-recipient of the Barry Carlton Award (best paper) of IEEE Transaction on Aerospace and Electronic Systems in 2001 and best paper award for the IEEE Transaction on Geoscience and Remote Sensing in 2003. He was with the technical committee of many international conferences on radar systems and signal processing. He was the Technical Committee Chairman of the IEEE/ISPRS Workshop on Remote Sensing and Data Fusion over Urban Areas URBAN'2001, Rome, URBAN'2003, Berlin, and URBAN'2005, Tempe (US). He was also the Technical Chairman of the IEEE Radar Conference 2008 in Rome and 2020 in Florence and Chairman of the European Radar Conference EuRAD'2022 in Milan. He is a Member of the Editorial board of IET Proceedings on Radar Sonar and Navigation.